DOI: 10.1002/ejoc.201100899

Synthesis and Glutathione Peroxidase-Like Activities of Isoselenazolines

Vijay P. Singh,[a] Harkesh B. Singh,*[a] and Ray J. Butcher[b]

Keywords: Heterocycles / Selenium / Ebselen / Antioxidants / Enzyme mimics / Structure–activity relationships

The aromatic nucleophilic substitution (S_NAr) reactions of *N*-(2-bromo-3-nitrobenzyl)aniline (**18**), *N*-(2-bromo-3-nitrobenzyl)-4-methylaniline (**19**) and *N*-(2-bromo-3-nitrobenzyl)-4-nitroaniline (**20**) with [*n*BuSeNa] afford *N*-[2-(butylselanyl)-3-nitrobenzyl]aniline (**21**), *N*-[2-(butylselanyl)-3-nitrobenzyl]-4-methylaniline (**22**) and *N*-[2-(butylselanyl)-3-nitrobenzyl]-4-nitroaniline (**23**), respectively. The bromination of **21** results in the formation of cyclic isoselenazolines 7-nitro-2-phenyl-2,3-dihydrobenzisoselenazole (**27**) and 2-(4-bromophenyl)-7-nitro-2,3-dihydrobenzisoselenazole (**28**). The bromination of **22** affords isoselenazolines 2-(4-methylphenyl)-7-nitro-2,3-dihydrobenzisoselenazole (**29**) and 2-(2-bromo-4-methylphenyl)-7-nitro-2,3-dihydrobenzisoselenazole (**30**) along with some other products. The bromination of **23** under identical conditions gave 2-(2-bromo-4-nitrophenyl)-7-nitro-2,3-dihydrobenzisoselenazole (**31**). The oxidation reaction of **21**–**22** with H_2O_2 yielded isoselenazoline *Se*-oxides 7-nitro-2-phenyl-2,3-dihydrobenzisoselenazole 1-oxide (**33**) and 2-(4-methylphenyl)-7-nitro-2-phenyl-2,3-dihydrobenzisoselenazole 1-oxide (**34**), respectively. The new isoselenazolines and isoselenazoline *Se*-oxides, stabilized by intramolecular secondary Se···O interactions, have been structurally characterized by single-crystal X-ray diffraction studies and investigated by computational studies. In addition to the synthesis and characterization, the glutathione peroxidase (GPx)-like activities of isoselenazolines and isoselenazoline *Se*-oxides have been evaluated by coupled reductase assays.

Introduction

Ebselen [2-phenyl-1,2-benzoselenzol-3(2*H*)-one, PZ 51, **1**], a heterocyclic compound containing a selenium–nitrogen bond, exhibits both anti-inflammatory activity in vivo and glutathione peroxidase (GPx)-like activity in vitro (Figure 1).[1] It catalytically reduces harmful peroxides by reducing glutathione (GSH) or other thiols, mimicking the activity of GPx and protecting the lipid membranes and other cellular components against oxidative damage.[2] Due to the applications of ebselen, several methods for its synthesis have been developed.[3,4] In the most direct approach, 2-(chlorocarbonyl)phenylselenenyl chloride obtained from 2,2′-diselenodibenzoic acid, is treated with aniline to afford ebselen.[4b] The method developed by Engman and coworkers involves *ortho*-lithiation of benzanilide followed by selenium insertion and oxidative cyclization reactions.[4c] A free radical synthesis of ebselen has been reported by intramolecular homolytic substitution with amidyl radicals.[4d,4e]

Very recently, an efficient copper-catalyzed method has been reported for ebselen.[5] The reactivity of ebselen could be interpolated by changing the basic structure based on substituent effects and isosteric replacements. To understand the effects of various substituents on the GPx activity of ebselen, several ebselen analogues have been reported.[6b,6d,6f] A pyridine-fused tocopherol and selenium containing antioxidant and anti-inflammatory agent **2** has been reported.[7] Selenenamide **3**, without an aromatic substituent, has also been developed as a model compound for GPx.[8] Another example of selenenamides such as **4**, containing a Se–N bond in the seven-membered ring has been reported.[9] The internalization of a subsidiary tetrahedral carbon atom (CR_2) into the heterocycle led to compounds **5**,[10] **6**[11] and **7**[12] as GPx mimics. It is worth mentioning that the introduction of an *ortho*-nitro group in 7-nitro-2-phenyl-1,2-benzoselenazol-3(2*H*)-one (**8**) enhances the GPx-like activity (Figure 2).[13] The synthesis of such eb-

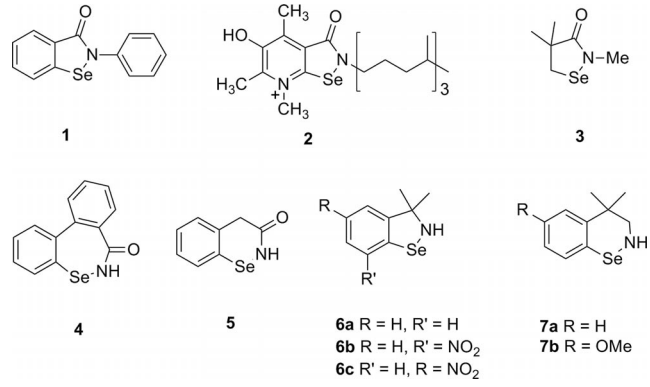

Figure 1. Ebselen (**1**) and its analogues **2**–**7**.

[a] Department of Chemistry, Indian Institute of Technology Bombay,
Powai, Mumbai 400076, India
Fax: +91-22-2572-3480
E-mail: chhbsia@chem.iitb.ac.in
[b] Department of Chemistry, Howard University, Washington, DC 20059, USA

Supporting information for this article is available on the WWW under http://dx.doi.org/10.1002/ejoc.201100899.

selen analogues **9**,[14a] **10**[14b] and **11**[14c] has been accomplished by *ortho*-lithiation and selenium insertion followed by oxidation. It has been revealed that the presence of intramolecular secondary Se···O/N interactions enhances the reactivity of the Se–N bond towards cleavage by thiols.[14c] The cyclic isoselenazolines, with a CH_2 group as part of the five-membered heterocyclic ring, have not been studied in detail. In contrast to ebselen, the isolation of such cyclic Se–N isoselenazolines is difficult due to the flexible –CH_2–NH– bond with a sp^3-hybridized carbon atom. To date, only a camphor-derived cyclic selenenamide **12**, which showed good GPx-like activity, has been reported (Figure 2).[15] Here, the cyclization could be possible due to the rigid conformation of the substrate. Furthermore, an attempted cyclization of 1-(bromomethyl)-2-(bromoseleno)-benzene with methylamine did not lead to the formation of the expected isoselenazoline **13**.[6d]

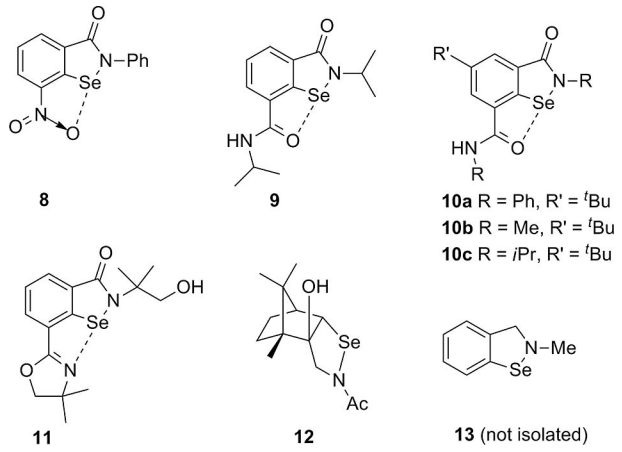

Figure 2. Selenenamides **8**–**12** and isoselenazoline **13**.

Recently, we have reported the synthesis of related Se–N heterocycles with imine (–CH=N–) and nitro (–NO_2) groups *ortho* to the selenium atom.[16] These heterocycles are closely related to ebselen and exhibit excellent GPx-like activity. We have now isolated a new range of Se–N heterocycles with a CH_2 group present in the five-membered ring. It occurred to us that such ebselen analogues might display interesting GPx-like activity due to a weaker Se–N bond. In this paper, we present our findings on the structure–property correlation as well as GPx-like activity of isoselenazolines and isoselenazoline *Se*-oxides with a CH_2 group and compare to analogues with a C=O group.

Results and Discussion

The precursor *N*-(2-bromo-3-nitrobenzylimino)benzene (**15**) was prepared from 2-bromo-3-nitrobenzaldehyde (**14**).[16] *N*-(2-Bromo-3-nitrobenzylimino)-4-methylaniline (**16**) and *N*-(2-bromo-3-nitrobenzylimino)-4-nitroaniline (**17**) were synthesized in a similar fashion by treating **14** with *p*-nitroaniline and *p*-toluidine, respectively (Scheme 1). Further treatment of **15**–**17** with $NaBH_4$ in ethanol afforded the expected reduced products **18**–**20** in good yields.

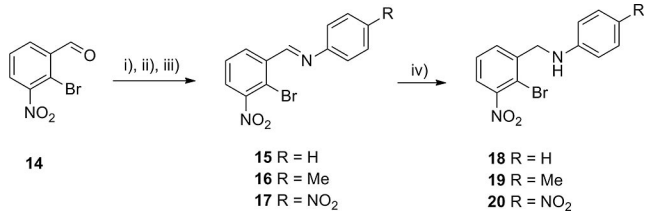

Scheme 1. i) Aniline, glacial acetic acid, r.t.; ii) *p*-toluidine, glacial acetic acid, r.t.; iii) *p*-nitroaniline, glacial acetic acid, r.t.; iv) $NaBH_4$, ethanol, r.t., 5 h.

Unsymmetrical selenides **21**–**23**, the required intermediates for the synthesis of isoselenazolines **27**–**31**, were synthesized by the aromatic nucleophilic substitution (S_NAr) reactions of **18**–**20** with the in situ prepared *n*BuSeNa (Scheme 2). Et_3N was added to a $CHCl_3$ solution of **21**. The progress of the reaction was monitored by TLC. After the usual work up, isoselenazolines **27** and **28** were obtained by silica gel column chromatographic purification with petroleum ether/ethyl acetate. Formation of **28** was accompanied by *N*-phenyl ring bromination at the *para*-position. To prevent the *N*-phenyl ring bromination at the *para*-position and to see the effect of the substituents when selenide **22** was treated with Br_2/Et_3N, the reaction mixture after work up and rotary evaporation afforded a black mixture of compounds, which was chromatographed on silca gel to afford isoselenazolines **29** and **30**, selenide **32** and another product,[17] respectively. A similar bromination reaction of **23** afforded isoselenazoline **31**, in very low yield, and a yellow precipitate, which could not be characterized.

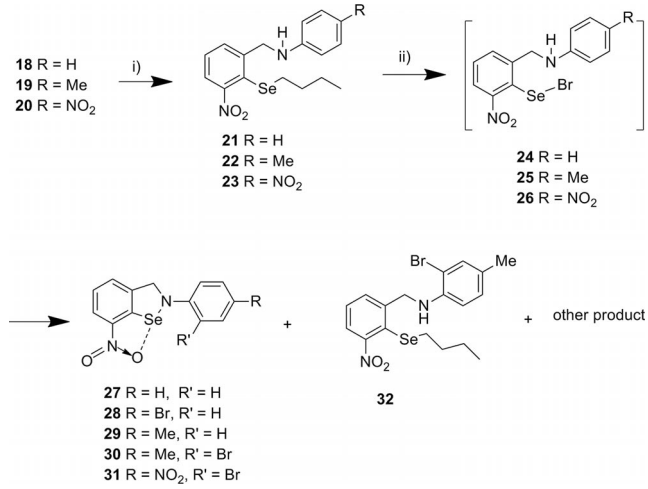

Scheme 2. i) [*n*BuSeNa], C_2H_5OH, 0 °C, 3 h; ii) $Br_2/CHCl_3$, Et_3N, 0 °C, 2 h.

To avoid bromination reactions in the cyclizations, oxidation with peroxides also leads to the cyclized products. The reaction of one equivalent as well as two equivalents of 30% H_2O_2 with selenides **21** and **22** at the room temperature did not lead to the formation of any products. Even

after adding six equivalents of H_2O_2 at room temperature with stirring for 24 h, only the starting materials were recovered. When the oxidation of **21** and **22** containing six equivalents of H_2O_2 was carried out with heating to reflux for 40–50 min, the reaction afforded the formation of over-oxidized isoselenazoline *Se*-oxides **33** and **34**, respectively (Scheme 3).

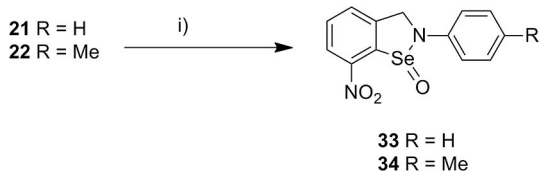

Scheme 3. i) Six equiv. of H_2O_2 (excess), $CHCl_3$, reflux, 40–50 min.

The reaction of selenides **21** and **22** with excess H_2O_2 presumably leads to selenoxides **35** and **36**, which undergo subsequent [2,3]-sigmatropic rearrangement to give selenenic acids **37** and **38** (Scheme 4). Furthermore, oxidation of **37** and **38** to seleninic acids **39** and **40** followed by condensation yields **33** and **34**.

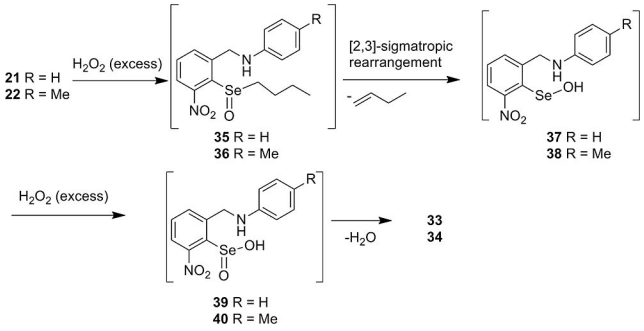

Scheme 4. Plausible mechanism for the formation of **33** and **34**.

In order to determine the structure–GPx-like activity correlations of the new cyclic isoselenazolines **27**–**31**, the related ebselen analogue **8** has also been prepared by a modified procedure.[13a] In our modification, 2-(butylselanyl)-3-nitro-*N*-phenylbenzamide (**42**), obtained by the reaction of 2-bromo-3-nitro-*N*-phenylbenzamide (**41**)[18] with in situ generated *n*BuSeNa, was used instead of 2-(methylselanyl)-3-nitro-*N*-phenylbenzamide (Figure 3).[13a] The reaction of **42** with Br_2/Et_3N in $CHCl_3$ solvent gave **8** in good yield.

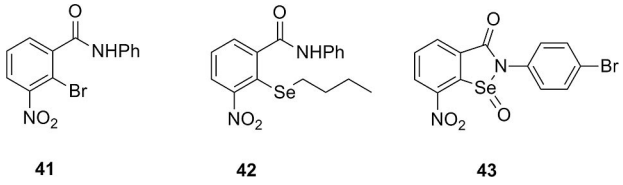

Figure 3. Precursors **41** and **42** and *ortho*-nitro-coordinating ebselen analogue **43**.

In summary, a facile synthesis of isoselenazolines and isoselenazoline *Se*-oxides incorporating a CH_2 group in the five-membered heterocyclic ring has been achieved. The intramolecular coordination of the 6-nitro group to the selenium atom plays a crucial role in the cyclization process.

Spectroscopic Studies

The ^{1}H NMR spectroscopic studies of **33** and **34** were performed in [D$_6$]DMSO (see Figures S92 and S99 of the Supporting Information). Nonequivalent signals for the benzylic protons of **33** [5.19 (d, 1 H) and 5.26 (d, 1 H) ppm] and **34** [5.16 (d, 1 H) and 5.24 (d, 1 H) ppm] were observed as two doublets with vicinal coupling (J = 16.0 Hz). The doublets are due the presence of the chiral selenium centres in optically active **33** and **34**.

^{77}Se NMR spectroscopy is a very useful technique for probing the electronic environment around the selenium atom.[6,8a,14–15,19a] The ^{77}Se NMR spectra of **27**–**31** exhibit signals at 974, 977, 987, 1060 and 1070 ppm (Table 1). These chemical shifts are slightly downfield compared to **1** (δ = 961 ppm),[6b] **8** (δ = 953 ppm),[13a] **3** (δ = 819 ppm),[8a] **7a** (δ = 693 ppm)[12b] and **12** (δ = 885 ppm).[15] As expected, the spectra of **33** and **34** with selenium(IV) showed larger downfield shifts than those of **27**–**31**.

Table 1. GIAO ^{77}Se NMR chemical shifts calculated in gas phase at the B3LYP/6-311+G(d,p) level on the B3LYP/6-311+G(d) level-optimized geometries for compounds **1**, **8**, **27**–**31** and **33**–**34** along with the experimental values.

Compound	^{77}Se NMR[a], calcd.	^{77}Se NMR[a], exp.	Solvents
1	988	961[6b]	$CDCl_3$
8	910	953[13a]	$CDCl_3$
27	992	974	$CDCl_3$
28	998	977	$CDCl_3$
29	997	987	$CDCl_3$
30	1074	1060	$CDCl_3$
31	1104	1070	$CDCl_3$
33	1161	1182	[D$_6$]DMSO
34	1158	1174	[D$_6$]DMSO

[a] The values are referenced to Me_2Se (δ = 0 ppm).

We performed DFT calculations on our organoselenium compounds to see the effect of a CH_2 group in place of the CO group in the five-membered heterocycle on the ^{77}Se NMR chemical shifts and compared the calculated values with the experimental data. The geometries were fully optimized with the B3LYP/6-311+G(d) basis sets. The NMR calculations were performed at the B3LYP/6-311+G(d,p) level on the B3LYP/6-311+G(d) level-optimized geometries by using the gauge-including atomic orbital (GIAO) method.[20] As observed from the experimental data, the calculated ^{77}Se NMR chemical shifts for **27**–**31** are downfield shifted compared to those observed for **1** (Table 1).

This difference in the chemical shifts is probably due to the presence of intramolecular secondary Se···O interactions with the *ortho*-nitro group. It is well established that the presence of the intramolecular secondary Se···N[6a,19b] and Se···O[6b,6e,21,22] interactions lead to a downfield shift of the ^{77}Se NMR chemical shifts. Recently, we have demonstrated that the presence of Se···O interactions in selenenium cations[16] and selenenate esters[22] leads to the downfield shift of the ^{77}Se NMR chemical shifts (vide infra).

Molecular Structures of 21 and 32

The molecular structure of **21** (Figure 4) shows a V-shaped geometry around the selenium atom with a C1–Se1–C14 bond angle of 100.00(11)°. The Se···O1 distance [3.295(9) Å] is slightly less than the sum of the van der Waals radii (3.45 Å), indicating a weak secondary Se···O interaction.[23] The geometry around the selenium atom in **32** is quite similar to that observed for **21** with a C1–Se1–C15A bond angle of 100.3(3)° (Figure 5). The Se···O2 distance [3.212(2) Å] is also similar to that observed for **21**.

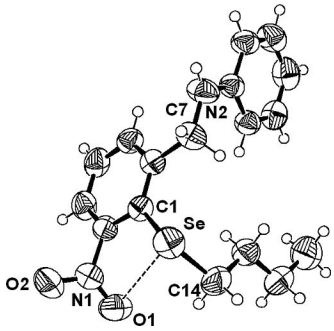

Figure 4. Molecular structure of **21**. Thermal ellipsoids are set at 50% probability. Significant bond lengths [Å] and angles [°]: Se···O1 3.295(9); Se–C1 1.924(2); Se–C14 1.978(3); O1···Se–C7 115.93(6); C1–Se–C14 100.00(11).

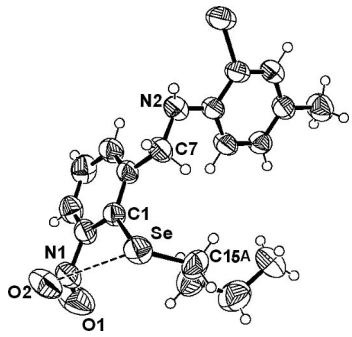

Figure 5. Molecular structure of **32**. Thermal ellipsoids are set at 50% probability. Significant bond lengths [Å] and angles [°]: Se···O2 3.212(2); Se–C11.926(3); Se–C15B 1.892(10); C1–Se–C14 100.3(3).

Molecular Structures of 29 and 30

The coordination geometry around the selenium atom in **29** is nearly T-shaped with a O1···Se–N2 bond angle of 156.76(11)° (Figure 6). The Se–N2 distance [1.891(3) Å] is similar to that reported for **1** [1.896(3) Å] and **8** [1.896(3)].[24] The Se···O1 distance [2.591(3) Å] is slightly greater than that reported for **8** [2.573(3) Å],[24b] which indicates a weak intramolecular secondary Se···O interaction in **29**. The geometry around the selenium atom in **30** is similar to that observed for **29** with a O1···Se–N2 bond angle of 155.61(10)° (Figure 7). The Se–N2 distance [1.905(3) Å] is similar to that observed in **29**. The Se···O1 distance [2.686(3) Å] is slightly greater than that observed in **30**, suggesting a weaker intramolecular secondary Se···O interaction.

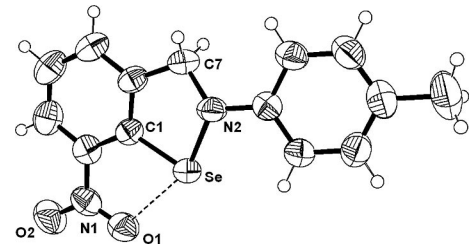

Figure 6. Molecular structure of **29**. Thermal ellipsoids are set at 50% probability. Significant bond lengths [Å] and angles [°]: Se···O1 2.591(3); Se–N2 1.891(3); Se–C1 1.861(3); O1···Se–N2 156.76(11); C1–Se–N2 85.69(14); C7–N2–Se 114.0(2).

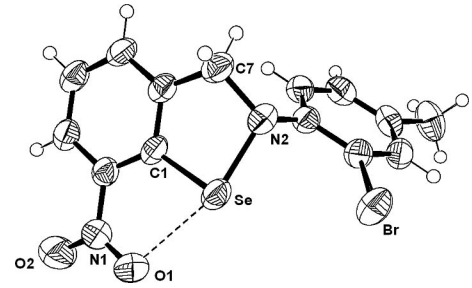

Figure 7. Molecular structure of **30**. Thermal ellipsoids are set at 50% probability. Significant bond lengths [Å] and angles [°]: Se···O1 2.686(3); Se–N2 1.905(3); Se–C1 1.880(3); O1···Se–N2 155.61(10); C1–Se–N2 88.11(12); C7–N2–Se 107.00(19).

Molecular Structure of 33

The molecular structure of **33** is shown in Figure 8. The geometry around the selenium shows a see-saw arrangement with a N2–Se···O2 bond angle of 152.31(16)°. This angle is quite similar to that reported for 2-(4-bromophenyl)-7-nitro-1,2-benzoselenazol-(*2H*)-3-one selenium oxide (**43**) [151.74(0)°].[16] The Se–N distance [1.867(4) Å] is slightly smaller than that observed in **43** [1.888(8) Å], and

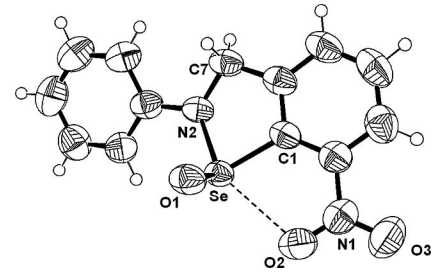

Figure 8. Molecular structure of **33**. Thermal ellipsoids are set at 50% probability. Significant bond lengths [Å] and angles [°]: Se···O2 2.742(5); Se–O1 1.645(4); Se–N2 1.867(4); Se–C1 1.938(6); N2–Se–C1 84.05(21); N2–Se···O2 152.31(16); N2–Se–O1 106.26(20); C1–Se–O1 104.33(21).

the Se···O2 distance [2.742(5) Å] is close to that observed in **43** (2.749 Å), indicating a weak secondary Se···O interaction.

Computational Studies

Effect of a CH_2 Group in Place of the CO Group in the Five-Membered Heterocycle

The reactivity of the Se–N bond in the ebselen analogues plays a crucial role in its GPx-like activity. The cleavage of the Se–N bond by the thiol leads to the formation of a Se–S bond.[6b,14c,25] Further attack by another thiol on the Se–S bond results in the formation of reactive selenol. The reactivity of the selenosulfide intermediate is tuned by intramolecular secondary Se···O interactions.[6,25] To study the effect of the incorporation of a CH_2 group in place of the C=O group and intramolecular secondary Se···O interactions on the nature of the Se–N bond in **27**–**31** and **33**–**34**, DFT calculations have been carried out (for the optimized geometries and coordinates see Tables S1, S3, S5, S7 and S9 of the Supporting Information). The data suggest that incorporation of the CH_2 group in place of the C=O group in **27**–**31** leads to an increase in the Se–N and Se···O distances (Table 2). In line with this observation, the Se–N distances in **1** (1.899 Å) and **8** (1.924 Å) are shorter compared with those in **27**–**31** and **33**–**34**.

Table 2. The theoretical data for **1**, **8**, **27**–**31** and **33**–**34** obtained by DFT calculations at the B3LYP/6-311+G(d,p) level. The NBO analysis was calculated at the B3LYP/6-311+G(d,p) level on the B3LYP/6-311+G(d) level-optimized geometries.

Compound	$r_{Se–N}$ [Å][a]	$r_{Se···O}$ [Å][a]	$E_{Se···O}$ [kcal/mol]	q_{Se}
1	1.899 (1.896)[24a]	–	–	+0.661
8	1.924 (1.896)[24b]	2.593 (2.573)	12.63	+0.753
27	1.939	2.605	11.96	+0.706
28	1.940	2.592	12.59	+0.709
29	1.941 (1.891)	2.613 (2.591)	11.53	+0.702
30	1.966 (1.905)	2.624 (2.686)	11.28	+0.701
31	1.967	2.514	19.13	+0.754
33	1.935 (1.867)	2.805 (2.742)	04.43	+1.562
34	1.934	2.809	04.30	+1.559

[a] The experimental values are given in parentheses.

The second-order perturbation energy ($E_{Se···O}$) between the selenium and oxygen atoms was calculated at the B3LYP/6-311+G(d,p) level on the B3LYP/6-311+G(d) level-optimized geometries using the natural bond orbital (NBO) calculations.[26] The $E_{Se···O}$ due to the $n_O \rightarrow \sigma^*_{Se–N}$ orbital interaction was obtained by NBO analysis. These studies reveal that with the replacement of C=O with a CH_2 group in **27**–**30** and **33**–**34** the $E_{Se···O}$ decreased slightly compared with that of **8** ($E_{Se···O}$ = 12.63 kcal/mol) suggesting a weaker Se···O interaction (Table 2). However, the $E_{Se···O}$ (19.13 kcal/mol) for **31** is found to be higher than for **8** and **27**–**30**, which is due to the presence of $–NO_2$ and –Br groups at the *N*-phenyl ring. The interaction energies for **33** ($E_{Se···O}$ = 04.43 kcal/mol) and **34** ($E_{Se···O}$ = 04.30 kcal/mol) are much lower compared with that of **27**–**31**, indicating weaker Se···O interactions in **33** and **34**. The NBO analysis further shows that weaker Se···O interactions and the presence of the CH_2 group lead to an elongation of the Se–N bond length.

Furthermore, distinct bond critical point (bcp) at the Se···O interaction correlates with the strength of the interacting atoms. The presence of bcp was identified in compounds **8**, **27**–**31** and **33**–**34** using Bader's theory of atoms in molecules (AIM)[27] with AIM2000 (Table 3).[28] The values of electron density (ρ) obtained are much smaller than that of a covalent bond (e.g., $\rho_{C–C}$ = 0.24 ea_0^{-3}) but larger than that of the practical boundary of molecules (ρ = 0.001 ea_0^{-3}).[29] The values of electron density $\rho_{Se···O}$ obtained for the Se···O interaction for **8**, **27**–**31** and **33**–**34** range from 0.020 to 0.034 ea_0^{-3} (see Figure S124 for AIM pictures in the Supporting Information). The trend of decreasing $\rho_{Se···O}$ from **27**–**30** to **33**–**34** is in accord with the trend of $E_{Se···O}$ obtained by the NBO analysis and the Se···O distance by quantum chemical calculation (Table 2). The Laplacian ($\nabla^2\rho_{Se···O}$) represents the curvature of electron density in 3D space at the bcp of the Se···O interaction. The values of $\nabla^2\rho_{Se···O}$ obtained for the Se···O interaction for **8**, **27**–**31** and **33**–**34** are all positive, suggesting a dominant electrostatic character. However, the total electron energy density ($H_{Se···O}$) is a more reliable measure for understanding the nature of secondary Se···O interactions instead of $\nabla^2\rho_{Se···O}$. The $H_{Se···O}$ values obtained for **27**–**30** and **33**–**34** are positive, which strongly suggests that the Se···O interactions are weak. It has been observed that the negative value of $H_{Se···O}$ for **31** indicates an increase in the strength of the Se···O interaction. The values obtained for **33**–**34** are found to be more positive than **8** and **27**–**30**. It is evident that the values of $H_{Se···O}$ become more positive with the increase in the Se···O atomic distance (i.e., weakening of the Se···O interaction). Similarly, positive values of $\nabla^2\rho_{Se···O}$ and total energy density $H_{Se···O}$ for Se···O interactions have been obtained by Tomoda and coworkers.[21a]

Table 3. Summary of properties of electron density at the bcp. Calculated at the B3LYP/6-311+G(d,p) level on the B3LYP/6-311+G(d) level-optimized geometries.

Compound	$\rho_{Se···O}$[a], (ea_0^{-3})	$\nabla^2\rho_{Se···O}$[b], (ea_0^{-5})	$H_{Se···O}$[c], (ea_0^{-4})
8	0.029	0.090	+0.0004
27	0.028	0.088	+0.0004
28	0.029	0.088	+0.0004
29	0.027	0.086	+0.0005
30	0.027	0.086	+0.0005
31	0.034	0.104	–0.0002
33	0.020	0.064	+0.0008
34	0.020	0.063	+0.0008

[a] The electron density at the bcp. [b] The Laplacian of the electron density at the bcp. [c] The total energy density at the bcp.

The NBO charge calculation shows that the Se···O interaction leads to an increased positive charge on the selenium atom in **8** (+0.753) than **1** (+0.661), which is due to the presence of an *ortho*-coordinating nitro group at the selenium atom. However, there is a slight decrease in the positive charge on the selenium atom of **27** (+0.706), **28** (+0.709), **29** (+0.702) and **30** (+0.701) compared to that of

8 (+0.753). It should be noted that the high positive charge on the selenium atom in **8** could be due to the delocalization of the carbonyl double bond in the five-membered heterocyclic ring as well as the *ortho*-coordinating nitro group. It has also been observed that the high positive charge on the selenium atom in **31** (+0.754) is due to the presence of the electron-withdrawing *para*-nitro group at the *N*-phenyl ring. Comparing **27**, **28**, **29**, **30** and **31** to **27**, with an unsubstituted *N*-phenyl ring, and **28**, **29**, **30** and **31**, substituted with –Br, –Me and $–NO_2$ groups at the *N*-phenyl ring, respectively, the high positive charge in **31** is found to be higher than that of **28**, **29** and **30**. This increase in the positive charge on the selenium atom in **31** is due to the *para*-nitro group at the *N*-phenyl ring. The positive charge on the selenium atom in **27**, **28**, **29** and **30** is found to be almost in the same range. As expected the NBO charges on the selenium atom in **33** (+1.562) and **34** (+1.559), which contain selenium(IV), are found to be higher than those of **1**, **8** and **27**–**31**.

The nucleus-independent chemical shift (NICS) value for **1** (–7.0 ppm) is more negative than that observed for **8** (–5.5 ppm) (see Table S19 of the Supporting Information). This significant loss in the aromatic character in the five-membered ring is due to the presence of the Se···O interaction and the conjugated carbonyl group. The Se···O interaction enhances the electrophilicty at the selenium atom. This decrease in the aromatic character from **27** (–2.4 ppm), **28** (–2.5 ppm), **29** (–2.5 ppm) and **30** (–3.0 ppm), **31** (–1.8 ppm), **33** (–1.6 ppm) and **34** (–1.7 ppm) is due the absence of the carbonyl group. The significant decrease in the NICS(0) values of **33**–**34** is mainly due to high positive charge on the selenium atom. Thus, the introduction of a CH_2 group in the five-membered heterocycle leads to a decrease in the aromaticity. In our earlier report,[22] similar behaviour for the carbonyl vs. CH_2 group has been observed in selenenate esters.

The results obtained by DFT calculations have shown that ^{77}Se NMR chemical shifts are shifted downfield in **27**–**31**, with a CH_2 group as part of the heterocycle, compared to that observed for **1** and **8** with a C=O group. Although the experimental Se–N bond lengths in **1**, **8**, **29**, **30** and **33** are in the same range, the calculated distances of **29**, **30** and **33** are much longer (i.e. lengthening of the Se–N bond) than those observed for **1** and **8**. These studies suggest that the introduction of a CH_2 group in place of the C=O group leads to the weakening of the Se–N bond and a decrease in the positive charge on the selenium atom as well as the aromaticity of the heterocycle.

Glutathione Peroxidase-Like Activity

The catalytic reduction of H_2O_2 using GSH as a cosubstrate in the presence and absence of catalysts **1**, **8**, **27**–**30** and **33**–**34** was studied (Table 4). The initial rates (ν_0) for the reduction were determined by the coupled reductase assay from a linear fit spanning the first 5–10% of the reaction by following the oxidation of reduced nicotinamide adenine dinucleotide (NADPH) at 340 nm in phosphate buffer. Interestingly, it was found that **29** (411 ± 1 μM min^{-1}), **33** (425 ± 1 μM min^{-1}) and **34** (506 ± 4 μM min^{-1}) exhibited much higher activities than the carbonyl group-based analogues **1** (133 ± 1 μM min^{-1}) and **8** (221 ± 2 μM min^{-1}). The GPx-like activity of **1** was found to be lower than **27**–**30**, which is due the absence of *ortho*-nitro group in **1**. The selenenyl sulfide derived from **1** has been shown to undergo thiol exchange reactions due to the presence of a strong Se···O interaction.[6] The strong Se···O interactions in selenosulfides hamper the generation of the reactive species selenol. Compound **8** showed nearly twice the activity of **1**. This enhancement in the GPx-like activity of **8** was due to the presence of an *ortho*-nitro group at the selenium atom.[13b] The GPx-like activity of **28** (204 ± 3 μM min^{-1}) was found to be higher than that of **27** (172 ± 5 μM min^{-1}) due to the presence of a *para*-substituent at the *N*-phenyl ring. Similarly, **29** showed better activity with a *para*-tolyl group at the heterocyclic N atom than **8**, **27**–**28** and **30** (255 ± 6 μM min^{-1}). The activity of **29** decreased to nearly half with an additional bromo substituent at the *ortho*-position of the *N*-phenyl ring. The high GPx-like activities of **33** and **34** are probably due to weak secondary Se···O interactions, lengthening of the Se–N bond and high positive charge on the selenium atom. The related ebselen analogue **43**[16] also showed good activity (472.7 ± 3.5 μM min^{-1}). In our earlier report,[22] it was observed that the seleninate esters exhibited much higher activity than selenenate esters. This study further suggests that the seleninamides **33**–**34** are even better catalysts than **27**–**30**. Similarly, *para*-substituted **28** and **29** were found to be better catalysts.

Table 4. Initial rates, ν_0 (μM min^{-1}) for the reduction of H_2O_2 by GSH in the presence of ebselen **1**, **8**, **27**–**30** and **33**–**34**.

Compound	ν_0 [μM min^{-1}][a]	Compound	ν_0 [μM min^{-1}][a]
Control[b,c]	31 ± 2	**29**	411 ± 1
1	133 ± 1	**30**	255 ± 6
8	221 ± 2	**33**	425 ± 1
27	172 ± 5	**34**	506 ± 4
28	204 ± 3	**43**	472.7 ± 3.5[d]

[a] Assay conditions: reactions were carried out with phosphate buffer (100 mM), pH 7.5, with ethylenediaminetetraacetate (EDTA): 1 mM; GSH: 2 mM; NADPH: 0.4 mM; glutathione reductase (GR): 1.3 unit/mL; selenium compounds: 80 μM; H_2O_2 (1.6 mM). [b] The control values were obtained from the reduction of H_2O_2 by GSH in the absence of selenium compounds. [c] All these values were triplicated for initial 10 s and average values were taken with standard deviation. [d] See ref.[16]

Determination of the Catalytic Parameters

To further understand the catalytic behaviour of **29** and **33**, which have good catalytic activities, detailed kinetic experiments were carried out. The Lineweaver–Burk (double reciprocal) plots for **1**, **29** and **33** (see Tables S29–S34 and Figures S125–S130 of the Supporting Information) were obtained by plotting the reciprocal of the initial rate ($1/\nu_0$) against the reciprocal of the substrate concentration

(1/[substrate]) and used for the determination of the catalytic parameters. The catalytic parameters, such as maximum velocity (V_{max}), Michaelis constant (K_M), catalytic constant (k_{cat}) and catalytic efficiency (η) were obtained for the reduction of H_2O_2 in the presence of **1**, **29** and **33** (Table 5). It is worth mentioning that the K_M values for **29** (2.05 mM) and **33** (0.93 mM) were lower than those obtained for **1** (14.47 mM) when GSH is variable, indicating that the thiol exchange reactions significantly increase the K_M values. The poor catalytic activity of ebselen has been ascribed to thiol exchange reactions in the selenenyl sulfide due to the presence of strong Se···O interactions.[6a–6c] The catalytic efficiencies of **29** and **33** were determined to be 3.83, 3.48 and 6.74, 8.34 $mM^{-1} min^{-1}$ respectively, whereas the catalytic efficiency of **1** was only 2.21, 0.61 $mM^{-1} min^{-1}$ when both H_2O_2 and GSH vary. The catalytic efficiency of **33** is ca. twice as high as that observed for **29**. The higher catalytic efficiency of **33** compared with **29** suggests that **33** is a more effective GPx mimetic than **29**, which may be due to fast reactions in the presence of thiol and peroxide. Moreover, in contrast to H_2O_2, typical saturation kinetics were observed at higher concentrations of GSH.

Table 5. Effect of H_2O_2 and GSH concentrations on V_{max}, K_M, k_{cat} and η for **1**, **29** and **33**.

Compound	V_{max} [$\mu M min^{-1}$]	K_M (mM)	k_{cat} [min^{-1}]	η [$mM^{-1} min^{-1}$]
Catalyst **1**				
H_2O_2 (variable)[a]	228.31	1.29	2.85	2.21
GSH (variable)[b]	709.22	14.47	8.86	0.61
Catalyst **29**				
H_2O_2 (variable)[a]	444.44	1.45	5.55	3.83
GSH (variable)[b]	571.43	2.05	7.14	3.48
Catalyst **33**				
H_2O_2 (variable)[a]	609.75	1.13	7.62	6.74
GSH (variable)[b]	621.12	0.93	7.46	8.34

[a] Assay conditions: Phosphate buffer (100 mM), pH 7.5; GSH: 2 mM; NADPH: 0.4 mM; EDTA: 1 mM; GR: 1 unit/mL; H_2O_2 (variable) and test compound: 80 μM. [b] Assay conditions: Phosphate buffer (100 mM), pH 7.5; GSH (variable), NADPH: 0.4 mM; EDTA: 1 mM; GR: 1 unit/mL; H_2O_2: 1.6 mM and test compound: 80 μM. For each value atleast two readings were taken.

Consumption of H_2O_2 by GSH in the Presence of 29 and 33

In order to prove that **29** and **33** behave as catalysts, kinetic reactions were followed until the completion of the reactions (maximum 10000 sec). Control experiments were carried out in the presence of H_2O_2 and GSH. A combination of catalysts (**29**/**33**), GSH and H_2O_2 was taken in a cuvette (containing 100 mM phosphate buffer pH 7.5, EDTA, NADPH and GR) and the decrease in the absorbance of NADPH was measured. A graph for the consumption for H_2O_2 vs. time was plotted from the data (see Tables S35–S37, Supporting Information). Up to 65 and 60% consumptions of H_2O_2 were observed after 70 and 166.66 min for **33** and **29**, respectively (Figure 9). This observation further shows that **33** is a better catalyst than **29**.

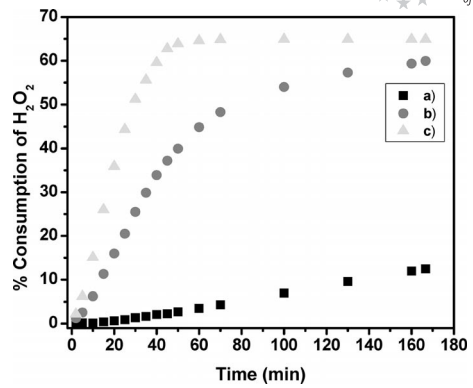

Figure 9. Catalytic reduction of H_2O_2 by GSH in the presence and absence of selenium catalyst. The consumption of H_2O_2 was followed by micromol of NADPH utilized per min: a) control i.e. in the absence of any catalyst; b) **29** + GSH + H_2O_2; c) **33** + GSH + H_2O_2. Assay conditions: reactions were carried out with phosphate buffer (100 mM), pH 7.5; with EDTA: 1 mM; GSH: 0.25 mM; NADPH: 0.40 mM; GR: 1.3 unit/mL; H_2O_2: 0.20 mM and selenium catalyst: 10 μM.

In summary, structure–activity correlations reveal that isoselenazolines **27**–**31** and isoselenazoline *Se*-oxides **33**–**34** with CH_2 groups are better GPx mimics than **1** and **8** with C=O groups. It has also been shown that **28** and **29** with *para*-substituents are nearly 1.5 and three times more active than **1**, respectively. As expected, **33** and **34** are significantly more active than their corresponding isoselenazolines **27** and **29**. To support the observations based on initial rates for **27** and **29** with a CH_2 group, further detailed kinetic studies using various concentrations of thiol and hydrogen peroxide indicate that compounds **29** and **33** are more efficient catalysts than **1**.

Catalytic Mechanism for 33

^{77}Se NMR spectroscopy was carried out to identify the intermediates involved in the catalytic mechanism of isoselenazoline *Se*-oxide **33** with promising GPx-like activity (Scheme 5). When **33** (δ = 1182 ppm) was treated with one equivalent of PhSH in [D_6]DMSO, a new signal was observed at δ = 973 ppm in addition to that of **33** (see Figures S131–S132, Supporting Information). The signal observed at δ = 973 ppm was assigned to isoselenazoline **27**. The identity of **27** was further established by its independent synthesis and complete characterization (see Experimental Section). Upon addition of one more equivalent of PhSH to the above mixture, both the signals at 1182 and 973 ppm completely disappeared and new signals were observed at 514 and 424 ppm (see Figures S133–S136 of the Supporting Information). These new signals at 514 and 424 ppm can be assigned to the corresponding selenosulfide **44** and diselenide **45**, respectively. The assignment of the signals at 514 and 424 ppm was further confirmed by the addition of two equivalents of PhSH to a solution of **27** in $CDCl_3$ (see Figure S137, Supporting Information). A similar observation has been made by Back and coworkers for the related selenenamide **12**, which follows a different catalytic mecha-

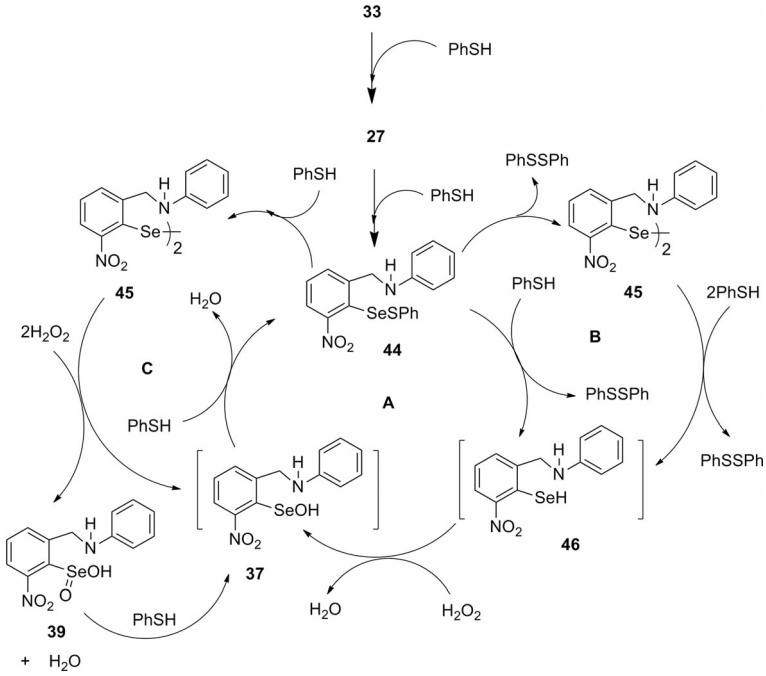

Scheme 5. Plausible catalytic cycle for the reduction of H_2O_2 by PhSH in the presence of **33**.

nism.[15] In the presence of more thiol, selenosulfide **44** was converted to disulfide (PhSSPh) and selenol **46** (Scheme 5, Cycle A). A ^{77}Se NMR signal for **46** was not observed in the catalytic cycle. Compound **46** probably oxidizes to selenenic acid **37**. Selenenic acid **37** reacted rapidly with PhSH to regenerate **44**. In the catalytic cycle, selenosulfide **44** disproportionates to the corresponding diselenide **45**. With excess thiol, diselenide **45** was converted to **46** (Scheme 5, Cycle B). The reaction of diselenide **45** with H_2O_2 may also produce the mixture of selenenic acid **37** and seleninic acid **39**. The rapid reaction of **45** with H_2O_2 produces **37** and **39** (Scheme 5, Cycle C). Interestingly, we did not observe the disproportionation of diselenide **45** with H_2O_2 to form **37** and **39**. Similar observations have been reported where the oxidation of diselenide with H_2O_2 produces a mixture of selenenic (ArSeOH) and seleninic acids ($ArSeO_2$ H).[6c–6e] In the presence of excess PhSH, both **37** and **39** produce the corresponding selenenyl sulfide **44**. The reaction of the in situ generated selenenic acids in the presence of PhSH leads to the formation of the corresponding selenenyl sulfides.[6e,15,25] On the basis of these observations, a plausible catalytic cycle for the reduction of **33** with H_2O_2 by PhSH has been proposed. The observation of diselenide **45** is in contrast to the mechanism reported by Back and coworkers for selenenamide **12**.[15]

Conclusions

An efficient methodology has been developed for the synthesis of new isoselenazolines incorporating a CH_2 moiety into the five-membered heterocyclic ring. The facile synthesis of isoselenazolines **27**–**31** and isoselenazoline *Se*-oxides **33**–**34** is due to the presence of an *ortho*-nitro group at the selenium atom. Theoretical investigations suggest that the replacement of the C=O group with a CH_2 group in the five-membered heterocycle activates the Se–N bond and decreases the positive charge on the selenium atom. It was observed that the selenium centre is more deshielded in the heterocycles with a CH_2 group, which may be due to weak intramolecular secondary Se···O interactions. Isoselenazoline **29** and isoselenazoline *Se*-oxides **33**–**34** exhibited excellent GPx-like activity.

Experimental Section

General: 2-Bromo-3-nitrobenzoic acid[30a] and 2-bromo-3-nitrobenzaldehyde[30b] were prepared by the reported procedures. Selenium powder and 3-nitrophthalic acid used were purchased from Sigma Aldrich. All the reactions were performed under nitrogen or argon atmosphere by modified Schlenk techniques and monitored by TLC. Silica gel of 100–200 mesh size was purchaged from merck. Solvents were purified by standard techniques.[31] Melting points were recorded with a VEEGO melting point (VMP1) apparatus and are uncorrected. ^{1}H NMR (399.88 MHz), ^{1}H (299.95 MHz), ^{13}C (100.6 MHz) and ^{77}Se (57.26 MHz) NMR spectra were recorded with a Varian NMR-Mercury plus 400 MHz, Bruker Avance^{III} 400 MHz spectrometer and Varian NMR-Mercury plus 300 MHz for ^{77}Se NMR at the indicated frequencies. Chemicals shifts (δ) are shown with respect to $SiMe_4$ as internal standard for nuclei ^{1}H and ^{13}C NMR and Me_2Se for ^{77}Se NMR as the external standard; s = singlet, d = doublet, t = triplet, dd = doublet of doublets, td = triplet of doublets. HRMS were recorded at room temperature with a Micro mass Q–TOF (YA 107) mass spectrometer. FTIR spectra were recorded in the range 4000–450 cm^{-1} using KBr for solid samples and CsI plates for liquid samples with a Perkin–Elmer precisely spectrum one FTIR spectrometer. The UV/VIS spectra for GPx-like activity in solution were recorded with a JASCO, V-570 spectrometer.

***N*-(2-Bromo-3-nitrobenzylimino)-4-methylaniline (16):** To a solution of **14** (43.4 mmol, 10.0 g) in glacial acetic acid (10 mL) was added *p*-toluidine (43.4 mmol, 4.64 g) with continuous stirring at room temperature. A curdy yellow precipitate was formed. To complete the precipitation, the reaction mixture was cooled with ice, then filtered and washed with ice-cooled ethanol. Recrystallization from hot ethanol afforded a light yellow solid; yield 8.9 g (65%); m.p. 110–112 °C. ^{1}H NMR ($CDCl_3$): δ = 2.39 (s, 3 H, CH_3), 7.19–7.24 (m, ArH), 7.52–7.56 (t, *J* = 7.9 Hz, 1 H), 7.77–7.80 (dd, *J* = 1.6, 9.51 Hz, 1 H), 8.42–8.45 (dd, *J* = 1.6, 9.5 Hz, 1 H), 8.92 (s, 1 H) ppm. ^{13}C NMR ($CDCl_3$): δ = 21.2, 116.7, 121.3, 126.7, 128.2, 130.1, 132.0, 137.3, 137.5, 148.2, 151.5, 156.4 ppm. IR (KBr): $\tilde{\nu}$ = 2918, 1616 (C=N), 1534 (NO_2), 1426, 1366, 1029, 829, 818, 713, 529, 487 cm^{-1}. HRMS (TOF MS ES$^+$) *m*/*z*: calcd. for $C_{14}H_{11}BrN_2O_2$ [M + H]$^+$: 319.0082; found 319.0088.

***N*-(2-Bromo-3-nitrobenzylimino)-4-nitroaniline (17):** Compound **17** was synthesized from **14** (8.69 mmol, 2.0 g) in glacial acetic acid (50 mL) and *p*-nitroaniline (8.69 mmol, 1.2 g) according to the procedure described for the preparation **16**; yield 1.6 g (53%); m.p. 195 °C. ^{1}H NMR ($CDCl_3$): δ = 7.30–7.32 (d, *J* = 1.9, 6.73 Hz, 2 H), 7.58–7.62 (t, *J* = 7.1 Hz, 1 H), 7.62–7.89 (dd, *J* = 1.6, 7.9 Hz, 1 H), 8.33–8.34 (d, *J* = 2.8 Hz, 2 H), 8.43–8.46 (dd, *J* = 1.6, 7.9 Hz, 2 H), 8.91 (s, 1 H) ppm. ^{13}C NMR ($CDCl_3$): δ = 117.5, 121.7, 125.3, 127.9, 128.6, 132.4, 136.4, 146.4, 151.7, 156.6, 160.3 ppm. IR (KBr): $\tilde{\nu}$ = 1601, 1582, 1532, 1514, 1341, 1107, 858, 738, 701 cm^{-1}. HRMS (TOF MS ES$^+$) *m*/*z*: calcd. for $C_{13}H_8BrN_3O_4$ [M + H]$^+$: 349.9776; found 349.9768.

General Procedure for the Synthesis of *sec*-Amine-Based Compounds 18–20: To a suspension of compounds **15**–**17** in ethanol (50 mL) was added $NaBH_4$ (4 equiv.) portionwise. The mixture was stirred for 5 h at room temperature under an inert atmosphere. The solvent was reduced to give a semisolid. The usual work up using water/chloroform afforded a yellow solution. The solvent was evaporated under reduced pressure to give yellow oil, which was solidified in the deep freeze to afford a crystalline solid.

***N*-(2-Bromo-3-nitrobenzyl)aniline (18):** Starting from **15** (9.8 mmol, 3.0 g); yield 2.4 g (80%); m.p. 110 °C. ^{1}H NMR ($CDCl_3$): δ = 4.34, (br. s, 1 H, NH), 4.48–4.49 (d, *J* = 4.9 Hz, 2 H, CH_2), 6.54–6.56 (dd, *J* = 1.0, 7.7 Hz, 2 H), 6.73–6.77 (td, *J* = 1.0, 7.4 Hz, 1 H), 7.16–7.20 (t, *J* = 7.7 Hz, 2 H), 7.35–7.39 (t, *J* = 7.7 Hz, 1 H), 7.59–7.62 (t, *J* = 6.6 Hz, 2 H) ppm. ^{1}H NMR (D_2O exchange): δ = 4.48 (s, 2 H, CH_2), 6.54–6.56 (m, 1 H), 6.73–6.74 (t, *J* = 7.7 Hz, 1 H), 7.16–7.20 (t, *J* = 7.7 Hz, 2 H), 7.35–7.39 (t, *J* = 7.7 Hz, 1 H), 7.59–7.62 (t, *J* = 6.6 Hz, 2 H) ppm. ^{13}C NMR ($CDCl_3$): δ = 48.9, 112.9, 114.0, 118.4, 123.6, 128.1, 129.5, 131.7, 141.7, 147.0, 151.2 ppm. IR (KBr): $\tilde{\nu}$ = 3412 (N–H), 3075, 3046, 3013, 2899, 1601, 1533, 1375, 1270, 755, 699 cm^{-1}. HRMS (TOF MS ES$^+$) *m*/*z*: calcd. for $C_{13}H_{11}BrN_2O_2$ [M + H]$^+$: 307.0082; found 307.0087.

***N*-(2-Bromo-3-nitrobenzyl)-4-methylaniline (19):** Starting from **16** (15.7 mmol, 5.0 g); yield 3.95 g (78%); m.p. 99–92 °C. ^{1}H NMR ($CDCl_3$): δ = 2.23 (s, 3 H, CH_3), 4.21 (br. s, 1 H, NH), 4.46 (s, 2 H, CH_2), 6.46–6.48 (d, *J* = 8.4 Hz, 2 H), 6.98–6.99 (d, *J* = 8.1 Hz, 2 H), 7.34–7.38 (t, *J* = 7.8 Hz, 1 H), 7.58–7.62 (t, *J* = 7.8 Hz, 2 H) ppm. ^{1}H NMR (D_2O exchange): δ = 2.23 (s, 3 H, CH_3), 4.46 (s, 2 H, CH_2), 4.80 (due to H_2O in D_2O), 6.46–6.48 (d, *J* = 8.4 Hz, 2 H), 6.98–6.99 (d, *J* = 8.1 Hz, 2 H), 7.34–7.38 (t, *J* = 7.8 Hz, 1 H), 7.58–7.62 (t, *J* = 7.8 Hz, 2 H) ppm. ^{13}C NMR ($CDCl_3$): δ = 20.5, 49.1, 113.0, 114.0, 123.6, 127.6, 128.1, 130.0, 131.7, 141.9, 144.8, 151.3 ppm. IR (KBr): $\tilde{\nu}$ = 3402, 3077, 2919, 1611, 1534, 1522, 1372, 1303, 1271, 825, 810, 797, 789 cm^{-1}. HRMS (TOF MS ES$^+$) *m*/*z*: calcd. for $C_{14}H_{13}BrN_2O_2$ [M + H]$^+$: 321.0239; found 321.0224.

***N*-(2-Bromo-3-nitrobenzyl)-4-nitroaniline (20):** Starting from **17** (5.2 mmol, 2.2 g); yield 1.35 g (61%); m.p. 162 °C. ^{1}H NMR ($CDCl_3$): δ = 4.60–4.62 (d, *J* = 6.3 Hz, 2 H, CH_2), 5.12–5.14 (t, NH), 6.54–6.57 (d, *J* = 7.9 Hz, 2 H), 7.42–7.45 (t, *J* = 7.4 Hz, 1 H), 7.50–7.52 (dd, 1 H), 7.65–7.67 (dd, 1 H), 8.08–8.11 (d, *J* = 8.9 Hz, 2 H) ppm. ^{13}C NMR ($CDCl_3$): δ = 48.3, 111.7, 144.4, 124.3, 126.5, 128.5, 131.2, 139.2, 139.8, 151.6, 152.4 ppm. IR (KBr): $\tilde{\nu}$ = 3364, 1601, 1529, 1309, 1284, 1112, 844 cm^{-1}. HRMS (TOF MS ES$^+$) *m*/*z*: calcd. for $C_{13}H_{10}BrN_3O_4$ [M + H]$^+$: 351.9933; found 351.9926.

General Method for the Synthesis of Unsymmetrical Selenides 21–23: To a solution of in situ prepared *n*BuSeNa (6.5 mmol) was added **18**–**20** (6.5 mmol) at 0 °C. The mixture was stirred for 3 h at room temperature under an inert atmosphere. The excess of the solvent was removed under reduced pressure to yield a yellow viscous solid, which was dissolved in $CHCl_3$ and then worked up. The combined organic layers were dried with anhydrous Na_2SO_4. The solvent was evaporated under reduced pressure and the product purified on silica gel column using ethyl acetate and petroleum ether (4%) as eluent to give an orange liquid.

***N*-[2-(Butylselanyl)-3-nitrobenzyl]aniline (21):** The compound was solidified in open air to afford yellow crystals; yield 0.85 g (36%); m.p. 63 °C. ^{1}H NMR ($CDCl_3$): δ = 0.86–0.90 (t, *J* = 7.3 Hz, 3 H), 1.33–1.42 (sext, *J* = 7.3 Hz, 2 H), 1.52–1.64 (quint, *J* = 7.3 Hz, 2 H), 2.84–2.88 (t, *J* = 7.3 Hz, 2 H), 4.30 (br. s, 1 H, NH), 4.65 (s, 2 H, CH_2), 6.56–6.58 (d, *J* = 8.1 Hz, 2 H), 6.72–6.76 (t, *J* = 7.3 Hz, 1 H), 7.16–7.20 (t, *J* = 7.3 Hz, 2 H), 7.37–7.41 (t, *J* = 7.7 Hz, 1 H), 7.48–7.50 (d, *J* = 6.9 Hz, 1 H), 7.64–7.66 (d, *J* = 7.3 Hz, 1 H) ppm. ^{1}H NMR (D_2O exchange): δ = 0.86–0.90 (t, *J* = 7.3 Hz, 3 H), 1.33–1.42 (sext, *J* = 7.3 Hz, 2 H), 1.52–1.64 (quint, *J* = 7.3 Hz, 2 H), 2.84–2.88 (t, *J* = 7.3 Hz, 2 H), 4.65 (s, 2 H, CH_2), 4.80 (due to H_2O in D_2O), 6.56–6.58 (d, *J* = 8.1 Hz, 2 H), 6.72–6.76 (t, *J* = 7.3 Hz, 1 H), 7.16–7.20 (t, *J* = 7.3 Hz, 2 H), 7.37–7.41 (t, *J* = 7.7 Hz, 1 H), 7.48–7.50 (d, *J* = 6.9 Hz, 1 H), 7.64–7.66 (d, *J* = 7.3 Hz, 1 H) ppm. ^{13}C NMR ($CDCl_3$): δ = 13.6, 22.9, 30.3, 32.5, 49.2, 112.9, 113.0, 118.1, 121.3, 121.9, 129.5, 130.6, 146.2, 147.4, 156.8 ppm. ^{77}Se NMR ($CDCl_3$): δ = 203 ppm. IR (KBr): $\tilde{\nu}$ = 3422, 2958, 2930, 1603, 1530, 1370, 1321, 1265, 802, 751 cm^{-1}. HRMS (TOF MS ES$^+$) *m*/*z*: calcd. for $C_{17}H_{20}N_2O_2Se$ [M + H]$^+$: 365.0768; found 365.0771.

***N*-[2-(Butylselanyl)-3-nitrobenzyl]-4-methylaniline (22):** Yield 1.46 g (78%). ^{1}H NMR ($CDCl_3$): δ = 0.86–0.90 (t, *J* = 0.1 Hz, 3 H), 1.34–1.39 (sext, *J* = 7.3 Hz, 2 H), 1.56–1.63 (quint, *J* = 7.9 Hz, 2 H), 2.23 (s, 3 H, CH_3), 2.84–2.88 (t, *J* = 7.5 Hz, 2 H), 4.17 (br. s, 1 H, NH), 4.62 (s, 2 H, CH_2), 6.48–6.51 (d, *J* = 8.3 Hz, 2 H), 6.97–6.99 (d, *J* = 8.3 Hz, 2 H), 7.38–7.47 (t, *J* = 6.2 Hz, 1 H), 7.46–7.49 (dd, *J* = 1.1, 7.9 Hz, 1 H), 7.63–7.65 (d, *J* = 7.5 Hz, 1 H) ppm. ^{1}H NMR (D_2O exchange): δ = 0.86–0.90 (t, *J* = 0.1 Hz, 3 H), 1.34–1.39 (sext, *J* = 7.3 Hz, 2 H), 1.56–1.63 (quint, *J* = 7.9 Hz, 2 H), 2.23 (s, 3 H, CH_3), 2.84–2.88 (t, *J* = 7.5 Hz, 2 H), 4.62 (s, 2 H, CH_2), 4.80 (due to H_2O in D_2O), 6.48–6.51 (d, *J* = 8.3 Hz, 2 H), 6.97–6.99 (d, *J* = 8.3 Hz, 2 H), 7.38–7.47 (t, *J* = 6.2 Hz, 1 H), 7.46–7.49 (dd, *J* = 1.1, 7.9 Hz, 1 H), 7.63–7.65 (d, *J* = 7.5 Hz, 1 H) ppm. ^{13}C NMR ($CDCl_3$): δ = 13.6, 20.5, 22.9, 30.3, 32.5, 49.5, 113.1, 121.2, 121.8, 127.3, 129.4, 129.9, 130.6, 145.1, 146.3, 156.8 ppm. ^{77}Se NMR ($CDCl_3$): δ = 203 ppm. IR (neat): $\tilde{\nu}$ = 3420 (N–H), 2958, 2929, 2870, 1617, 1523, 1370, 808 cm^{-1}. HRMS (TOF MS ES$^+$) *m*/*z*: calcd. for $C_{18}H_{22}N_2O_2Se$ [M + H]$^+$: 379.0925; found 379.0916.

***N*-[2-(Butylselanyl)-3-nitrobenzyl]-4-nitroaniline (23):** Compound **23** was purified on silica gel column using ethyl acetate and petroleum ether (10%) as eluent to give an orange liquid. This was solidified in open air to give a dark green solid; yield 0.80 g (46%); m.p.

88 °C. ^{1}H NMR ($CDCl_3$): δ = 0.86–0.90 (t, J = 7.3 Hz, 3 H), 1.32–1.40 (sext, J = 7.3 Hz, 2 H), 1.56–1.64 (quint, J = 7.6 Hz, 2 H), 2.85–2.89 (t, J = 7.6 Hz, 2 H), 4.77 (s, 2 H, CH_2), 5.31 (br. s, 1 H, NH), 6.55–6.57 (d, J = 9.2 Hz, 2 H), 7.42–7.46 (t, J = 7.6 Hz, 1 H), 7.52–7.54 (d, J = 7.6 Hz, 1 H), 7.57–7.59 (d, J = 7.6 Hz, 1 H), 8.05–8.05 (d, J = 8.9 Hz, 2 H) ppm. ^{13}C NMR ($CDCl_3$): δ = 13.6, 22.9, 30.7, 32.5, 48.6, 111.7, 121.7, 122.5, 126.5, 129.9, 130.5, 138.8, 144.7, 152.7, 157.0 ppm. ^{77}Se NMR ($CDCl_3$): δ = 206 ppm. IR (KBr): $\tilde{\nu}$ = 3354, 2950, 2926, 2868, 1602, 1525, 1300, 1105, 834 cm^{-1}. HRMS (TOF MS ES$^+$) m/z: calcd. for $C_{17}H_{19}N_3O_4Se$ [M + H]$^+$: 410.0619; found 410.0631.

General Procedure for the Synthesis of 27 and 28: To a solution of **21** (2.75 mmol, 1.0 g), in dry $CHCl_3$ (2 mL) was added Br_2 (0.18 mL, 3.30 mmol) in $CHCl_3$ (2 mL) over 30 min at 0 °C under an inert atmosphere. After the bromination was complete, triethylamine (2.75 mmol, 0.27 g, 0.38 mL) was added to the reaction mixture. The reaction was stirred at room temperature for 2 h. The mixture was extracted into $CHCl_3$ by adding water (10 mL). The organic layers were combined and dried with anhydrous Na_2SO_4. Removal of solvent and purification of the residue by silica gel column chromatography (eluted with 2% ethyl acetate/petroleum ether mixture) afforded **27** and **28**.

7-Nitro-2-phenyl-2,3-dihydro-1,2-benzoselenazole (27): Compound **27** was recrystallized from dichloromethane/diethyl ether to give a dark purple solid; yield 0.06 g (7%); m.p. 146 °C (dec.). ^{1}H NMR ($CDCl_3$): δ = 5.04 (s, 2 H), 6.70–6.99 (m, 2 H), 7.27–7.29 (m, 1 H), 7.38–7.42 (t, J = 7.9 Hz, 1 H), 7.59–7.61 (d, J = 7.3 Hz, 1 H), 8.19–8.21 (d, J = 8.3 Hz, 1 H) ppm. ^{13}C NMR ($CDCl_3$): δ = 60.0, 116.6, 120.2, 123.5, 127.2, 128.3, 129.5, 139.1, 141.7, 143.1, 151.2 ppm. ^{77}Se NMR ($CDCl_3$): δ = 974 ppm. IR (KBr): $\tilde{\nu}$ = 2925, 1595, 1511, 1293, 733 cm^{-1}. HRMS (TOF MS ES$^+$) m/z calcd. for $C_{13}H_{10}N_2O_2Se$ [M + H]$^+$: 306.9986; found 306.9977.

2-(4-Bromophenyl)-7-nitro-2,3-dihydro-1,2-benzoselenazole (28): Recrystallization from dichloromethane/diethyl ether afforded **28** as a dark purple solid; yield 0.37 g (35%); m.p. 155 °C (dec.). ^{1}H NMR ($CDCl_3$): δ = 5.00 (s, 2 H, CH_2), 6.67–6.69 (d, J = 8.8 Hz, 2 H), 7.33–7.36 (d, J = 9.2 Hz, 2 H), 7.39–7.44 (t, J = 7.7 Hz, 1 H), 7.58–7.61 (d, J = 8.3 Hz, 1 H), 8.19–8.21 (d, J = 8.1 Hz, 1 H) ppm. ^{13}C NMR ($CDCl_3$): δ = 59.9, 112.3, 117.9, 123.6, 127.4, 128.4, 132.2, 138.6, 141.2, 142.9, 150.0 ppm. ^{77}Se NMR ($CDCl_3$): δ = 977 ppm. IR (KBr): $\tilde{\nu}$ = 1589, 1570, 1514, 1286, 801 cm^{-1}. HRMS (TOF MS ES$^+$) m/z: calcd. for $C_{13}H_9BrN_2O_2Se$ [M + H]$^+$: 384.9091; found 384.9091.

General Procedure for the Synthesis of 29–30 and 32: To a solution of **22** (4.29 mmol, 1.62 g) in dry $CHCl_3$ (20 mL) was added bromine (4.29 mmol, 0.68 g, 222 µL) and Et_3N (4.29 mmol, 0.433 g, 594 µL) at 0 °C according to the procedure described for the preparation of **27**. Removal of the solvent and purification of the residue by silica gel column chromatography (eluted with 2–6% ethyl acetate/petroleum ether) afforded **29**–**30** and **32**.

7-Nitro-2-*p*-tolyl-2,3-dihydro-1,2-benzoselenazole (29): Recrystallization from dichloromethane/ether afforded a dark black compound; yield 0.05 g (3%); m.p. 140 °C. ^{1}H NMR ($CDCl_3$): δ = 2.27 (s, 3 H, CH_3), 4.99 (s, 2 H, CH_2), 6.7–6.8 (d, J = 8.5 Hz, 2 H), 7.05–7.07 (d, J = 8.6 Hz, 2 H), 7.37–7.41 (t, J = 7.9 Hz, 1 H), 7.60–7.62 (d, J = 7.3 Hz, 1 H), 8.17–8.19 (d, J = 7.3 Hz, 1 H) ppm. ^{13}C NMR ($CDCl_3$): δ = 20.6, 61.0, 117.3, 123.4, 127.2, 128.2, 129.9, 130.5, 139.3, 142.1, 143.3, 149.7 ppm. ^{77}Se NMR ($CDCl_3$): δ = 987 ppm. IR (KBr): $\tilde{\nu}$ = 2916, 2855, 1615, 1511, 1287, 799, 730 cm^{-1}. HRMS (TOF MS ES$^+$) m/z: calcd. for $C_{14}H_{13}N_2O_2Se$ [M + H]$^+$: 321.0142; found 321.0145.

2-(2-Bromo-4-methylphenyl)-7-nitro-2,3-dihydro-1,2-benzoselenazole (30): Recrystallization from chloroform/ether afforded orange crystals; yield 0.05 g (3%); m.p. 165 °C. ^{1}H NMR ($CDCl_3$): δ = 2.24 (s, 3 H, CH_3), 4.98 (s, 2 H, CH_2), 6.79–6.87 (m, 2 H), 7.42 (s, 1 H), 7.44–7.47 (t, J = 7.3 Hz, 1 H), 7.69–7.72 (dd, J = 1.1, 7.3 Hz, 1 H), 8.17–8.19 (d, J = 7.7 Hz, 1 H) ppm. ^{13}C NMR ($CDCl_3$): δ = 20.5, 63.3, 119.2, 119.6, 123.6, 127.5, 127.9, 128.7, 134.3, 135.5, 139.8, 143.7, 144.2, 150.8 ppm. ^{77}Se NMR ($CDCl_3$): δ = 1060 ppm. IR (KBr): $\tilde{\nu}$ = 3082, 2919, 1598, 1508, 1315, 824 cm^{-1}. HRMS (TOF MS ES$^+$) m/z: calcd. for $C_{14}H_{11}BrN_2O_2Se$ [M + H]$^+$: 398.9247; found 398.9232.

2-Bromo-*N*-[2-(butylselanyl)-3-nitrobenzyl]-4-methylaniline (32): Recrystallization from chloroform/ether afforded yellow crystals; yield 0.35 g (19%); m.p. 58 °C. ^{1}H NMR ($CDCl_3$): δ = 0.86–0.91 (t, J = 7.4 Hz, 3 H), 1.32–1.43 (sext, J = 7.2 Hz, 2 H), 1.56–1.64 (quint, J = 5.4 Hz, 2 H), 2.21 (s, 3 H, CH_3), 2.84–2.87 (t, J = 7.6 Hz, 2 H), 4.68–4.69 (s, 2 H, CH_2), 4.82–4.85 (br. s, 1 H, NH), 6.33–6.35 (d, J = 8.2 Hz, 1 H), 6.89–6.92 (dd, J = 1.5, 8.2 Hz, 1 H), 7.28–7.30 (dd, J = 0.6, 1.0 Hz, 1 H), 7.37–7.41 (t, J = 7.9 Hz, 1 H), 7.47–7.50 (dd, J = 1.8, 7.8 Hz, 1 H), 7.57–7.59 (dd, J = 0.7, 7.8 Hz, 1 H) ppm. ^{13}C NMR ($CDCl_3$): δ = 13.6, 20.2, 22.9, 30.4, 32.5, 49.2, 109.8, 111.7, 121.4, 122.0, 128.3, 129.2, 129.6, 130.3, 133.0, 141.9, 145.7, 156.9 ppm. ^{77}Se NMR ($CDCl_3$): δ = 203 ppm. IR (KBr): $\tilde{\nu}$ = 3394 (N–H), 2967, 2925, 1606, 1509, 1365, 803 cm^{-1}. HRMS (TOF MS ES$^+$) m/z: calcd. for $C_{18}H_{21}N_2O_2SeBr$ [M + H]$^+$: 457.0030; found 457.0016.

2-(2-Bromo-4-nitrophenyl)-7-nitro-2,3-dihydro-1,2-benzoselenazole (31): To a solution of **23** (1.95 mmol, 0.8 g), in dry $CHCl_3$ (210 mL) was added bromine (1.9 mmol, 0.31 g, 100 µL) and Et_3N (1.95 mmol, 0.19 g, 270 µL) at 0 °C according to the procedure described for the preparation of **27**. The reaction mixture was filtered and the filtrate was reduced to give a dark red semisolid, which was purified by column chromatography with silica gel (eluted with 10% ethyl acetate/petroleum ether) to afford **31** as a brown powder; yield 0.005 g (0.6%); m.p. 170–174 °C. ^{1}H NMR ($CDCl_3$): δ = 5.04 (s, 2 H, CH_2), 7.00–7.02 (d, J = 8.8 Hz, 1 H), 7.49–7.53 (t, J = 7.6 Hz, 1 H), 7.76–7.79 (d, J = 7.4 Hz, 1 H), 7.98–8.01 (dd, J = 2.2, 8.9 Hz, 1 H), 8.21–8.23 (d, J = 7.9 Hz, 1 H), 8.48–8.49 (d, J = 2.2 Hz, 1 H) ppm. ^{77}Se NMR ($CDCl_3$): δ = 1070 ppm. IR (KBr): $\tilde{\nu}$ = 1591, 1495, 1315, 1112, 735 cm^{-1}. HRMS (TOF MS ES$^+$) m/z: calcd. for $C_{13}H_8BrN_3O_4Se$ [M + H]$^+$: 429.8940; found 429.8942.

7-Nitro-2-phenyl-2,3-dihydro-1,2-benzoselenazole 1-Oxide (33): To a solution of **21** (3.30 mmol, 1.20 g) in $CHCl_3$ (5 mL) was added 30% H_2O_2 (19.82 mmol, 2.2 mL) at room temperature. The reaction was stirred for 25 min at room temperature and then heated at 55–60 °C for 40–50 min. The orange precipitate formed was collected by filtration and dried under vacuum to give orange solid **33**. The product was recrystallized from DMSO/diethyl ether to afford dark red needle-like crystals; yield 0.42 g (40%); m.p. 164 °C. ^{1}H NMR ([D$_6$]DMSO): δ = 5.17–5.22 (d, J = 16.0 Hz, 1 H), 5.24–5.29 (d, J = 16.0 Hz, 1 H), 6.98–7.03 (t, J = 7.3 Hz, 1 H), 7.21–7.24 (d, J = 7.7 Hz, 2 H), 7.35–7.40 (t, J = 7.3 Hz, 2 H), 7.93–7.98 (t, J = 7.7 Hz, 1 H), 8.13–8.15 (d, J = 7.7 Hz, 1 H), 8.37–8.40 (d, J = 8.1 Hz, 1 H) ppm. ^{13}C NMR ([D$_6$]DMSO): δ = 55.9, 116.8, 121.3, 123.8, 129.9, 132.1, 133.2, 140.5, 144.0, 144.6, 145.2 ppm. ^{77}Se NMR ([D$_6$]DMSO): δ = 1182 ppm. IR (KBr): $\tilde{\nu}$ = 3081, 2823, 1594, 1531, 1341, 823, 814, 748 cm^{-1}. HRMS (TOF MS ES$^+$) m/z: calcd. for $C_{14}H_{10}N_2O_3Se$ [M + H]$^+$: 322.9935; found 322.9932.

7-Nitro-2-*p*-tolyl-2,3-dihydro-1,2-benzoselenazole 1-Oxide (34): Compound **34** was synthesized from **22** (1.32 mmol, 0.50 g), $CHCl_3$ (2 mL) and 30% H_2O_2 (7.96 mmol, 0.90 mL) according to the procedure described for the preparation of **33**. The red precipitate ob-

tained was collected by filtration and dried under vacuum. The product was recrystallized from DMSO/diethyl ether to afford dark red crystals; yield 0.18 g (38%); m.p. 156–158 °C. ^{1}H NMR ([D$_6$]DMSO): δ = 2.27 (s, 3 H, CH$_3$), 5.14–5.19 (d, J = 16.0 Hz, 1 H), 5.22–5.27 (d, J = 16.0 Hz, 1 H), 7.12–7.15 (d, J = 8.7 Hz, 2 H), 7.18–7.21 (d, J = 8.7 Hz, 2 H), 7.95–7.97 (t, J = 7.8 Hz, 1 H), 8.12–8.15 (d, J = 7.8 Hz, 1 H), 8.37–8.39 (d, J = 7.8 Hz, 1 H) ppm. ^{13}C NMR ([D$_6$]DMSO): δ = 20.1, 55.9, 117.2, 123.6, 130.1, 130.4, 131.9, 132.9, 142.8, 141.9, 143.9, 145.3 ppm. ^{77}Se NMR ([D$_6$]-DMSO): δ = 1174 ppm. IR (KBr): $\tilde{\nu}$ = 3091, 2824, 1570, 1530, 1340, 1280, 827, 733 cm^{-1}. HRMS (TOF MS ES$^+$) m/z: calcd. for $C_{14}H_{12}N_2O_3Se$ [M + H]$^+$: 337.0091; found 337.0087.

2-Bromo-3-nitro-*N*-phenylbenzamide (41): To a mixture of thionyl chloride (50 mL) and DMF (1 mL) was added 2-bromo-3-nitrobenzoic acid[30a] (40.0 mmol, 10.0 g) and the mixture was heated to reflux for 3–4 h. The excess thiony chloride was removed under vacuum applying a liquid N$_2$ trap. The brown precipitate obtained was dissolved in dichloromethane. Aniline (100 mmol, 10 mL) in dry dichloromethane was added dropwise to a suspension of the brown precipitate at room temperature over 2–3 h, and the reaction was stirred at room temperature for overnight. The mixture was extracted into dichloromethane by adding water (10 mL). The organic layers were combined and dried with anhydrous Na$_2$SO$_4$. The solvent was evaporated under reduced pressure to give yellow oil, which was solidified in the deep freeze to give a crystalline solid **41**; yield 6.5 g (50%); m.p. 153–155 °C. ^{1}H NMR (CDCl$_3$): δ = 7.18–7.23 (t, J = 7.3 Hz, 1 H), 7.36–7.41 (t, J = 7.3 Hz, 2 H), 7.50–7.55 (t, J = 7.8 Hz, 1 H), 7.59–7.61 (d, J = 7.3 Hz, 2 H), 7.68–7.71 (dd, J = 1.5, 7.8 Hz, 1 H), 7.45–7.78 (dd, J = 1.5, 7.8 Hz, 1 H) ppm. ^{13}C NMR (CDCl$_3$): δ = 111.6, 120.4, 125.6, 126.2, 128.9, 129.4, 131.9, 137.2, 141.2, 151.2, 164.4 ppm. IR (KBr): $\tilde{\nu}$ = 3289 (NH), 1661, 1528, 1369, 1326, 755 cm^{-1}. HRMS (TOF MS ES$^+$) m/z: calcd. for $C_{13}H_9BrN_2O_3$ [M + H]$^+$: 320.9875; found 320.9873.

2-(Butylselanyl)-3-nitro-*N*-phenylbenzamide (42): Compound **42** was synthesized from **41** (6.22 mmol, 2.0 g) with in situ prepared *n*BuSeNa (6.22 mmol, 0.24 g) in deoxygenated ethanol according to the procedure described for the preparation of **21**–**23**. Removal of solvent and purification of the residue by silica gel column chromatography (eluted with 10% ethyl acetate/petroleum ether mixture) afforded **42** as a yellow solid; yield 1.2 g (53%); m.p. 98 °C. ^{1}H NMR (CDCl$_3$): δ = 0.74–0.79 (t, J = 7.3 Hz, 3 H),1.19–1.31 (sext, J = 7.3 Hz, 2 H), 1.45–1.55 (quint, J = 7.3 Hz, 2 H), 2.85–2.89 (t, J = 7.3 Hz, 2 H), 7.18–7.22 (t, J = 7.3 Hz, 1 H), 7.38–7.43 (t, J = 8.3 Hz, 2 H), 7.49–7.54 (t, J = 7.8 Hz, 1 H), 7.64–7.66 (d, J = 6.8 Hz, 2 H), 7.82–7.87 (dd, J = 1.5, 6.8 Hz, 1 H), 7.88–7.91 (dd, J = 1.5, 6.8 Hz, 1 H), 8.35 (s, 1 H, NH) ppm. ^{13}C NMR (CDCl$_3$): δ = 13.5, 22.7, 31.1, 31.9, 119.9, 122.4, 125.3, 125.6, 128.9, 129.4, 133.3, 137.6, 142.8, 155.0, 165.4 ppm. ^{77}Se NMR (CDCl$_3$): δ = 276 ppm. IR (KBr): $\tilde{\nu}$ = 3294 (NH), 1658 (CO), 1520, 1436, 1324, 748, 713 cm^{-1}. HRMS (TOF MS ES$^+$) m/z: calcd. for $C_{17}H_{18}N_2O_3$ Se [M + H]$^+$: 379.0561; found 379.0546.

7-Nitro-2-phenyl-1,2-benzoselenazol-3(2*H*)-one (8): To a solution of **42** (0.53 mmol, 0.40 g), in dry CHCl$_3$ (5 mL) was added bromine (0.53 mmol, 0.084 g, 0.027 mL) and triethylamine (0.53 mmol, 0.053 g, 0.072 mL) according to the procedure described for the preparation of **27**. Removal of solvent and purification of the residue by silica gel column chromatography (eluted with 10% ethyl acetate/petroleum ether mixture) afforded **8**; yield 0.31 g (92%, lit.[13a] 78%); m.p. 168–170 °C (lit. 160–163 °C). ^{1}H NMR (CDCl$_3$): δ = 7.30–7.35 (t, J = 7.3 Hz, 2 H), 7.45–7.50 (t, J = 8.6 Hz, 2 H) 7.63–7.65 (d, J = 7.3 Hz, 1 H), 7.71–7.76 (t, J = 7.8 Hz, 1 H), 8.46–8.49 (dd, J = 1.0, 7.7 Hz, 1 H), 8.57–8.60 (dd, J = 1.0, 8.3 Hz, 1 H) ppm. ^{13}C NMR (CDCl$_3$): δ = 125.1, 127.2, 127.7, 127.9, 129.7, 131.5, 135.3, 136.4, 138.5, 142.1, 163.9 ppm. ^{77}Se NMR (CDCl$_3$): δ = 924 ppm. IR (KBr): $\tilde{\nu}$ = 1650 (CO), 1607, 1518 (NO$_2$), 1298, 751, 736 cm^{-1}. HRMS (TOF MS ES$^+$) m/z: calcd. for $C_{13}H_8N_2O_3Se$ [M + H]$^+$: 320.9778; found 320.9769.

Coupled Reductase Assay: GPx-like activity of the organoselenium compounds was determined by a spectrophotometric method at 340 nm described by Wilson et al.[32] The test mixture contained GSH (2 mM), EDTA (1 mM), glutathione reductase (1.3 unit/mL) and NADPH (0.4 mM) in 100 mM potassium phosphate buffer, pH 7.5. GPx samples (80 μM) were added to the test mixture at 25 °C and the reaction was started by the addition of H$_2$O$_2$ (1.6 mM). The initial reduction rates were calculated from the oxidation rate of NADPH at 340 nm. The initial reduction rate was determined at least 3–4 times and calculated from the first 5–10% of the reaction using 6.22 mM^{-1}cm^{-1} as the extinction coefficient for NADPH.

X-ray Crystallographic Analysis: X-ray crystallographic studies were carried out for **21**, **29**–**30** and **32**–**33** with a Oxford Diffraction Gemini diffractometer using graphite-monochromatized Mo-K_α radiation λ = 1.54184 Å for **21**, **29**–**30** and **32**–**33**. The diffraction measurements were performed at 295(2) K. The structures were solved by direct method and refined by a full-matrix least-squares procedure on F^2 for all reflections with SHELXL-97 software.[33] Hydrogen atoms were localized by geometrical means. A riding model was chosen for refinement. The isotropic thermal parameters of hydrogen atoms were fixed at 1.5 times for (CH$_3$ groups) or 1.2 times U(eq) (Ar-H) of the corresponding carbon atoms. Some details of the refinement are given in Tables 6 and 7.

Table 6. Crystal data and structure refinement for **21**, **29** and **30**.

	21	**29**	**30**
Empirical formula	$C_{17}H_{20}N_2O_2Se$	$C_{14}H_{12}N_2O_2Se$	$C_{14}H_{11}BrN_2O_2Se$
Formula weight	363.31	319.22	398.12
Crystal system	triclinic	monoclinic	monoclinic
Space group	$P\bar{1}$	$P12_1/c1$	$P12_1/c1$
a [Å]	8.1599(5)	13.6944(6)	13.0789(2)
b [Å]	10.1630(6)	6.3988(3)	7.80369(12)
c [Å]	11.0254(8)	15.6904(8)	13.9947(2)
α [°]	93.953(6)	90	90
β [°]	107.286(6)	106.224(5)	98.9459(16)
γ [°]	99.356(5)	90	90
V [Å^3]	854.71(10)	1320.17(11)	1410.97(4)
Z	2	4	4
$D_{calcd.}$ [Mg/m^3]	1.412	1.606	1.874
Abs. coeff. [mm^{-1}]	3.041	3.854	6.951
Obsd. reflections [$I > 2\sigma(I)$]	6633	5302	6152
Final $R(F)$ [$I > 2\sigma(I)$][a]	0.0381	0.0503	0.0325
$wR(F^2)$ indices [$I > 2\sigma(I)$]	0.1071	0.1404	0.0848
Data / restraints / parameters	3567 / 0 / 204	2736 / 0 / 173	2942 / 0 / 183
Goodness of fit on F^2	1.039	1.060	1.043

[a] Definitions: $R(F_o) = ||F_o| - |F_c||/|F_o|$ and $wR(F_o^2) = \{\Sigma[w(F_o^2 - F_c^2)^2]/[w(F_c^2)^2\}^{1/2}$.

CCDC-808887 (for **21**), -808888 (for **33**), -808890 (for **32**), -808891 (for **29**) and -808892 (for **30**) contain the supplementary crystallographic data for this paper. These data can be obtained free of charge from The Cambridge Crystallographic Data Centre via www.ccdc.cam.ac.uk/data_request/cif.

Table 7. Crystal data and structure refinement for **32** and **33**.

	32	**33**
Empirical formula	$C_{18}H_{21}BrN_2O_2Se$	$C_{13}H_{10}N_2O_3Se$
Formula weight	456.24	321.19
Crystal system	monoclinic	orthorhombic
Space group	$P12_11$	*Pbcn*
a [Å]	10.9761(5)	13.1780(4)
b [Å]	8.0108(2)	8.4675(3)
c [Å]	11.7412(5)	22.6182(8)
α [°]	90	90
β [°]	113.054(5)	90
γ [°]	90	90
V [Å^3]	949.93(7)	2523.85(15)
Z	2	8
$D_{calcd.}$ [Mg/m^3]	1.595	1.691
Abs. coeff. [mm^{-1}]	5.240	4.100
Obsd. reflections [$I > 2\sigma(I)$]	6828	21353
Final $R(F)$ [$I > 2\sigma(I)$][a]	0.0333	0.0635
$wR(F^2)$ indices [$I > 2\sigma(I)$]	0.0937	0.1407
Data / restraints / parameters	3575 / 1 / 238	2659 / 0 / 172
Goodness of fit on F^2	1.062	1.179

[a] Definitions: $R(F_o) = ||F_o| - |F_c||/|F_o|$ and $wR(F_o^2) = \{\Sigma[w(F_o^2 - F_c^2)^2]/[w(F_c^2)^2\}^{1/2}$.

Computational Methods: All theoretical calculations were executed using the Gaussian 03 suite of quantum chemical programs.[34] The hybrid Becke 3-Lee–Yang–Parr (B3LYP) exchange correlation functional was implemented for DFT calculations.[35] The geometry optimizations were carried out at the B3LYP level of DFT by using the 6-311+G(d) basis sets. The total energies of the optimized geometries were computed based on with inclusion of zero-point corrections. The ^{77}Se NMR calculations were performed at B3LYP/6-311+G(d,p) level on B3LYP/6-311+G(d)-level optimized geometries using the gauge-including atomic orbital (GIAO) method (referenced with respect to the peak of Me_2Se).[20] The quantifications of orbital interaction were preformed by NBO analysis at the B3LYP/6-311+G(d,p) level.[26] AIM[27–29] calculations were used to confirm distinct bond critical point. NICS[36] were carried out at the B3LYP/6-311+G(d)//6-311+G(d,p) level.

Supporting Information (see footnote on the first page of this article): ^{1}H NMR, ^{13}C NMR, ^{77}Se NMR, HR mass and IR spectra of all the newly synthesized compounds, tables for GPx-like activity, coordinates, NBO charges, NBO second-order perturbation energies, AIM pictures for optimized geometries of compounds **8**, **27**–**31** and **33**–**34**.

Acknowledgments

This work was supported by the Department of Science and Technology (DST), New Delhi. We are thankful to the Sophisticated Analytical Instrument facility (SAIF), Indian Institute of Technology (IIT), Bombay, for performing 300 MHz NMR spectroscopic analyses for ^{77}Se NMR spectroscopy. V. P. S. wishes to thank IIT Bombay for a teaching assistantship.

[1] a) A. Müller, E. Cadenas, P. Graf, H. Sies, *Biochem. Pharmacol.* **1984**, *33*, 3235–3239; b) A. Wendel, M. Fausel, H. Safayhi, G. Tiegs, R. Otter, *Biochem. Pharmacol.* **1984**, *33*, 3241–3245; c) M. J. Parnham, S. Kindt, *Biochem. Pharmacol.* **1984**, *33*, 3247–3250; d) A. Müller, H. Gabriel, H. Sies, *Biochem. Pharmacol.* **1985**, *34*, 1185–1189; e) H. Safayhi, G. Tiegs, A. Wendel, *Biochem. Pharmacol.* **1985**, *34*, 2691–2694; f) A. Wendel, European Patent 0–165–534, **1985**; g) A. Wendel, G. Tiegs, *Biochem. Pharmacol.* **1986**, *35*, 2115–2118; h) T. Schewe, *Gen. Pharmacol.* **1995**, *26*, 1153–1169; i) M. J. Parnham, H. Sies, *Expert Opin. Invest. Drugs* **2000**, *9*, 607–619; j) G. Mugesh, H. B. Singh, *Chem. Soc. Rev.* **2000**, *29*, 347–357; k) G. Mugesh, W.-W. du Mont, H. Sies, *Chem. Rev.* **2001**, *101*, 2125–2179.

[2] a) L. Flohè, E. A. Günzler, H. H. Schock, *FEBS Lett.* **1973**, *32*, 132–134; b) J. T. Rotruck, A. L. Pope, H. E. Ganther, A. B. Swanson, D. G. Hafeman, W. G. Hoekstra, *Science* **1973**, *179*, 588–590; c) C. Jacob, G. I. Giles, N. M. Giles, H. Sies, *Angew. Chem. Int. Ed.* **2003**, *42*, 4742–4758.

[3] R. Lesser, R. Weiss, *Ber. Dtsch. Chem. Gen.* **1924**, *57*, 1077–1082.

[4] a) R. Weber, M. Renson, *Bull. Soc. Chim. Fr.* **1976**, 1124–1126; b) A. Welter, L. Christiaens, P. Wirtz, Eur. Pat. Appl. EP 44453, **1982**; c) L. Engman, A. Hallberg, *J. Org. Chem.* **1989**, *54*, 2964–2966; d) M. C. Fong, C. H. Schiesser, *Tetrahedron Lett.* **1995**, *36*, 7329–7332; e) M. C. Fong, C. H. Schiesser, *J. Org. Chem.* **1997**, *62*, 3103–3108.

[5] S. J. Balkrishna, B. S. Bhakuni, D. J. Chopra, K. Sangit, *Org. Lett.* **2010**, *12*, 5394–5397.

[6] a) B. K. Sarma, G. Mugesh, *J. Am. Chem. Soc.* **2005**, *127*, 11477–11485; b) K. P. Bhabak, G. Mugesh, *Chem. Eur. J.* **2007**, *13*, 4594–4601; c) B. K. Sarma, G. Mugesh, *Chem. Eur. J.* **2008**, *14*, 10603–10614; d) K. P. Bhabak, G. Mugesh, *Chem. Eur. J.* **2009**, *15*, 9846–9854; e) K. P. Bhabak, G. Mugesh, *Chem. Asian J.* **2009**, *4*, 974–983; f) K. Satheeshkumar, G. Mugesh, *Chem. Eur. J.* **2011**, *17*, 4849–4857.

[7] T. Fenner, C. H. Schiesser, *Molecules* **2004**, *9*, 472–479.

[8] a) H. J. Reich, C. P. Jasperse, *J. Am. Chem. Soc.* **1987**, *109*, 5549–5551; b) P. Cotelle, P. Chan, N. Cotelle, J. L. Bernier, J. P. Henichart, *J. Chim. Phys.-Chim. Biol.* **1992**, *89*, 191–198.

[9] A. Mohsine, L. Christiaens, *Heterocycles* **1996**, *43*, 2567–2593.

[10] P. V. Jacquemin, L. E. Christiaens, M. J. Renson, M. J. Evers, N. Dereu, *Tetrahedron Lett.* **1992**, *33*, 3863–3866.

[11] J. Chaudiere, I. Erdelmeier, M. Moutet, J.-C. Yadan, *Phosphorus Sulfur Silicon Relat. Elem.* **1998**, *136*, *137 & 138*, 467–470.

[12] a) J. Chaudière, J.-C. Yadan, I. Erdelmeier, C. Tailhan-Lomont, M. Moutet, in: *Oxidative processes and Antioxidants* (Ed.: R. Paoletti), Ravan Press, New York, **1994**, p. 165; b) I. Erdelmeier, M. Moutet, J.-C. Yadan, *J. Org. Chem.* **2000**, *65*, 8152–8157.

[13] a) C. Lambert, L. Christiaens, *Tetrahedron* **1991**, *47*, 9053–9060; b) M. J. Parnham, J. Biedermann, Ch. Bittner, N. Dereu, S. Leyck, H. Wetzig, *Agents Actions* **1989**, *27*, 306–308; c) B. Dakova, L. Lamberts, M. Evers, N. Dereu, *Electrochim. Acta* **1991**, *36*, 631–637; d) J. K. Pearson, R. J. Boyd, *J. Phys. Chem. A* **2008**, *112*, 1013–1017.

[14] a) B. Kersting, M. DeLion, *Z. Naturforsch., Teil B* **1999**, *54*, 1042–1047; b) S. S. Zade, S. Panda, S. K. Tripathi, H. B. Singh, G. Wolmershauser, *Eur. J. Org. Chem.* **2004**, 3857–3864; c) G. Roy, G. Mugesh, *J. Am. Chem. Soc.* **2005**, *127*, 15207–15217.

[15] T. G. Back, B. P. Dyck, *J. Am. Chem. Soc.* **1997**, *119*, 2079–2083.

[16] V. P. Singh, H. B. Singh, R. J. Butcher, *Eur. J. Inorg. Chem.* **2010**, 637–647.

[17] V. P. Singh, H. B. Singh, R. J. Butcher, *Chem. Commun.* **2011**, *47*, 7221–7223.

[18] A. Burger, A. C. Schmalz, *J. Org. Chem.* **1954**, *19*, 1841–1846.

[19] a) M. Iwaoka, T. Katsuda, H. Komatsu, S. Tomoda, *J. Org. Chem.* **2005**, *70*, 321–327; b) M. Iwaoka, S. Tomoda, *J. Am. Chem. Soc.* **1996**, *118*, 8077–8084.

[20] C. A. Bayse, *Inorg. Chem.* **2004**, *43*, 1208–1210.

[21] a) M. Iwaoka, H. Komatsu, T. Katsuda, S. Tomoda, *J. Am. Chem. Soc.* **2004**, *126*, 5309–5317; b) W. Nakanishi, S. Hayashi, S. Toyota, *Chem. Commun.* **1996**, 371; c) W. Nakanishi, S. Hayashi, A. Sakaue, G. Ono, Y. Kwada, *J. Am. Chem. Soc.* **1998**, *120*, 3635–3640.

[22] V. P. Singh, H. B. Singh, R. J. Butcher, *Chem. Asian J.* **2011**, *6*, 1431–1442 and references cited therein.

[23] A. Bondi, *J. Phys. Chem.* **1964**, *68*, 441–445.

[24] a) L. Dupont, O. Dideberg, P. Jacqemin, *Acta Crystallogr., Sect. C* **1990**, *46*, 484–486; b) L. Dupont, O. Dideberg, M. Sbit, N. Dereu, *Acta Crystallogr., Sect. C* **1988**, *44*, 2159–2161.
[25] K. P. Bhabak, G. Mugesh, *Chem. Eur. J.* **2008**, *14*, 8640–8651.
[26] a) A. E. Reed, L. A. Curtiss, F. Weinhold, *Chem. Rev.* **1988**, *88*, 899–926; b) F. Weinhold, *Natural Bond Orbital (NBO)*, version 5.0.
[27] R. W. F. Bader, *Atoms in Molecules: A Quantum Theory*, Oxford University Press, New York, **1990**.
[28] F. Beigler-Konig, J. Schonbohm, D. Bayles, *J. Comput. Chem.* **2001**, *22*, 545–559.
[29] P. Popelier, *Atoms In Molecules: An Introduction*; Pearson, Harlow, **2000**.
[30] a) F. C. Whitmore, P. J. Culhane, *J. Am. Chem. Soc.* **1929**, *51*, 602–605; b) L. K. A. Rahman, R. M. Scrowston, *J. Chem. Soc. Perkin Trans. 1* **1984**, 385–390.
[31] D. D. Perrin, W. L. F. Armarego, *Purification of Labratory Chemicals*, Pergamon Press, 4th ed., **1996**.
[32] S. R. Wilson, P. A. Zucker, R.-R. C. Huang, A. Spector, *J. Am. Chem. Soc.* **1989**, *111*, 5936–5939.
[33] G. M. Sheldrick, *SHELXL-97*, Program for Crystal Structure Determination, University of Göttingen, Germany, **1974**.
[34] M. J. Frisch, G. W. Trucks, H. B. Schlegel, G. E. Scuseria, M. A. Robb, J. R. Cheeseman, J. A. Montgomery Jr., T. Vreven, K. N. Kudin, J. C. Burant, J. M. Millam, S. S. Iyengar, J. Tomasi, V. Barone, B. Mennucci, M. Cossi, G. Scalmani, N. Rega, G. A. Petersson, H. Nakatsuji, M. Hada, M. Ehara, K. Toyota, R. Fukuda, J. Hasegawa, M. Ishida, T. Nakajima, Y. Honda, O. Kitao, H. Nikai, M. Klene, X. Li, J. E. Knox, H. P. Hratchian, J. B. Cross, V. Bakken, C. Adamo, J. Jaramillo, R. Gomperts, R. E. Stratmann, O. Yazyev, A. J. Austin, R. Commi, C. Pomelli, J. W. Ochterski, P. Y. Ayala, K. Morokuma, G. A. Voth, P. Salvador, J. J. Dannenberg, V. G. Zakrazewski, S. Dapprich, A. D. Daniels, M. C. Strain, O. Farkas, D. K. Malick, A. D. Rabuck, K. Raghabachari, J. B. Foresman, J. V. Ortiz, Q. Cui, A. G. Baboul, S. Clifford, J. Cioslowski, B. B. Stefanov, G. Liu, A. Liashenko, P. Piskorz, I. Komaromi, R. L. Martin, D. J. Fox, T. Keith, M. A. Al-Laham, C. Y. Peng, A. Nanayakkara, M. Challacombe, P. M. W. Gill, B. Johnson, W. Chen, M. W. Wong, C. Gonzalez, J. A. Pople, *Gaussian 03*, rev. C.02, Gaussian, Inc., Wallingford, CT, **2004**.
[35] a) C. Lee, W. Yang, R. G. Parr, *Phys. Rev. B* **1988**, *37*, 785–789; b) A. D. Becke, *J. Chem. Phys.* **1993**, *98*, 5648–5652.
[36] a) P. von Rague Schleyer, C. Maerker, A. Dransfeld, H. Jiao, N. J. R. van Eikema Hommes, *J. Am. Chem. Soc.* **1996**, *118*, 6317–6318; b) P. von Rague Schleyer, M. Manoharan, Z.-X. Wang, B. Kiran, H. Jiao, R. Puchta, N. J. R. van Eikema Hommes, *Org. Lett.* **2001**, *3*, 2465–2468; c) Z. Chen, C. S. Wannere, C. Corminboeuf, R. Puchta, P. von Rague Schleyer, *Chem. Rev.* **2005**, *105*, 3842–3888; d) E. Kleinpeter, S. Klod, A. Koch, *THEOCHEM* **2007**, *811*, 45–60.

Received: June 20, 2011
Published Online: August 10, 2011

